

## Collective Modes in Light Nuclei from First Principles

T. Dytrych,<sup>1</sup> K. D. Launey,<sup>1</sup> J. P. Draayer,<sup>1</sup> P. Maris,<sup>2</sup> J. P. Vary,<sup>2</sup> E. Saule,<sup>3,\*</sup> U. Catalyurek,<sup>3,4</sup> M. Sosonkina,<sup>5</sup>  
D. Langr,<sup>6</sup> and M. A. Caprio<sup>7</sup>

<sup>1</sup>*Department of Physics and Astronomy, Louisiana State University, Baton Rouge, Louisiana 70803, USA*

<sup>2</sup>*Department of Physics and Astronomy, Iowa State University, Ames, Iowa 50011, USA*

<sup>3</sup>*Department of Biomedical Informatics, The Ohio State University, Columbus, Ohio 43210, USA*

<sup>4</sup>*Department of Electrical and Computer Engineering, The Ohio State University, Columbus, Ohio 43210, USA*

<sup>5</sup>*Department of Modeling, Simulation and Visualization Engineering, Old Dominion University, Norfolk, Virginia 23529, USA*

<sup>6</sup>*Department of Computer Systems, Faculty of Information Technology, Czech Technical University in Prague, Prague 16000, Czech Republic*

<sup>7</sup>*Department of Physics, University of Notre Dame, Notre Dame, Indiana 46556, USA*

(Received 25 April 2013; published 18 December 2013)

Results for *ab initio* no-core shell model calculations in a symmetry-adapted SU(3)-based coupling scheme demonstrate that collective modes in light nuclei emerge from first principles. The low-lying states of <sup>6</sup>Li, <sup>8</sup>Be, and <sup>6</sup>He are shown to exhibit orderly patterns that favor spatial configurations with strong quadrupole deformation and complementary low intrinsic spin values, a picture that is consistent with the nuclear symplectic model. The results also suggest a pragmatic path forward to accommodate deformation-driven collective features in *ab initio* analyses when they dominate the nuclear landscape.

DOI: [10.1103/PhysRevLett.111.252501](https://doi.org/10.1103/PhysRevLett.111.252501)

PACS numbers: 21.60.Cs, 21.60.De, 21.60.Fw, 27.20.+n

*Introduction.*—Major progress in the development of realistic internucleon interactions along with the utilization of massively parallel computing resources [1–3] have placed *ab initio* approaches [4–14] at the frontier of nuclear structure explorations. The ultimate goal of *ab initio* studies is to establish a link between underlying principles of quantum chromodynamics (quark or gluon considerations) and observed properties of atomic nuclei, including their structure and related reactions. The predictive potential that *ab initio* models hold [15,16] makes them suitable for targeting short-lived nuclei that are inaccessible by experiment but essential to modeling, for example, of the dynamics of x-ray bursts and the path of nucleosynthesis (see, e.g., Refs. [17,18]).

In this Letter, we report on *ab initio* symmetry-adapted no-core shell model (SA-NCSM) results for the <sup>6</sup>Li (odd-odd), <sup>8</sup>Be (even-even), and <sup>6</sup>He (halo) nuclei, using two realistic nucleon-nucleon (*NN*) interactions, the JISP16 [19] and chiral N<sup>3</sup>LO [20] potentials. The SA-NCSM framework exposes a remarkably simple physical feature that is typically masked in other *ab initio* approaches: the emergence, without *a priori* constraints, of simple orderly patterns that favor spatial configurations with strong quadrupole deformation and low intrinsic spin values. This feature, once exposed and understood, can be used to guide a truncation and augmentation of model spaces to ensure that important properties of atomic nuclei, like enhanced *B(E2)* strengths, nucleon cluster substructures, and others important in reactions, are appropriately accommodated in future *ab initio* studies.

The SA-NCSM joins a no-core shell model (NCSM) theory [4] with a multishell, SU(3)-based coupling scheme

[21,22]. Specifically, nuclear wave functions are represented as a superposition of many-particle configurations carrying a particular intrinsic quadrupole deformation linked to the irreducible representation (irrep) labels ( $\lambda\mu$ ) of SU(3) [23–25], and specific intrinsic spins ( $S_p S_n S$ ) for protons, neutrons, and total spin, respectively (proton-neutron formalism). The fact that SU(3) plays a key role, e.g., in the microscopic description of the experimentally observed collectivity of *ds*-shell nuclei [26–30], and for heavy deformed systems [31], tracks from the seminal work of Elliott [21] and is reinforced by the fact that it is the underpinning symmetry of the microscopic symplectic model [32,33], which provides a comprehensive theoretical foundation for understanding the dominant symmetries of nuclear collective motion [29,34].

The outcome further suggests a symmetry-guided basis selection that yields results that are nearly indistinguishable from the complete basis counterparts. This is illustrated for <sup>6</sup>Li and <sup>6</sup>He for a range of harmonic oscillator energies  $\hbar\Omega$ , and  $N_{\max} = 12$  model spaces, where  $N_{\max}$  is the maximum number of harmonic oscillator quanta included in the basis states above the Pauli allowed minimum for a given nucleus. An overarching long-term objective is to extend the reach of the standard NCSM scheme by exploiting symmetry-guided principles that enable one to include configurations beyond the  $N_{\max}$  cutoff, while capturing the essence of long-range correlations that often dominate the nuclear landscape.

*Ab initio realization of collective modes.*—The expansion of eigenstates in the physically relevant SU(3) basis unveils salient features that emerge from the complex dynamics of these strongly interacting many-particle systems. To explore the nature of the most important correlations, we

analyze the probability distribution across  $(S_p S_n S)$  and  $(\lambda\mu)$  configurations of the four lowest-lying isospin-zero ( $T = 0$ ) states of  ${}^6\text{Li}$  ( $1_{\text{gs}}^+$ ,  $3_1^+$ ,  $2_1^+$ , and  $1_2^+$ ), along with the ground-state rotational bands of  ${}^8\text{Be}$  and  ${}^6\text{He}$ . Results for the ground state of  ${}^6\text{Li}$  and  ${}^8\text{Be}$ , obtained with the JISP16 and chiral  $\text{N}^3\text{LO}$  interactions, respectively, are shown in Fig. 1. This figure illustrates a feature common to all the low-energy solutions considered: namely, a highly structured and regular mix of intrinsic spins and SU(3) spatial quantum numbers that has heretofore gone unrecognized in other *ab initio* studies, and which does not seem to depend on the particular choice of realistic  $NN$  potential.

First, consider the spin content. The calculated eigenstates project at a 99% level onto a comparatively small subset of intrinsic spin combinations. For instance, the lowest-lying eigenstates in  ${}^6\text{Li}$  are almost entirely realized in terms of configurations characterized by the following intrinsic spin  $(S_p S_n S)$  triplets:  $(\frac{3}{2} \frac{3}{2} 3)$ ,  $(\frac{1}{2} \frac{3}{2} 2)$ ,  $(\frac{3}{2} \frac{1}{2} 2)$ , and  $(\frac{1}{2} \frac{1}{2} 1)$ , with the last one carrying over 90% of each eigenstate. Similarly, the ground-state bands of  ${}^8\text{Be}$  and  ${}^6\text{He}$  are found to be dominated by configurations carrying total intrinsic spin of the protons and neutrons equal to zero and one, with the largest contributions due to  $(S_p S_n S) = (000)$  and  $(112)$  configurations.

Second, consider the spatial degrees of freedom. The mixing of  $(\lambda\mu)$  quantum numbers exhibits a remarkably simple pattern. One of its key features is the preponderance of a single  $0\hbar\Omega$  SU(3) irrep. This irrep, termed leading irrep, is characterized by the largest value of the intrinsic quadrupole deformation [23]; for instance, the low-lying states of  ${}^6\text{Li}$  project at a 40%–70% level onto the prolate  $0\hbar\Omega$  SU(3) irrep (20), as illustrated in Fig. 1. For the ground state band of  ${}^8\text{Be}$  and  ${}^6\text{He}$ , qualitatively similar dominance of the leading  $0\hbar\Omega$  SU(3) irreps is observed. The dominance of the most deformed  $0\hbar\Omega$  configuration indicates that the quadrupole-quadrupole interaction of the Elliott SU(3) model [21] is realized naturally within an *ab initio* framework.

The analysis also reveals that the dominant SU(3) basis states at each  $N\hbar\Omega$  subspace ( $N = 0, 2, 4, \dots$ ) are typically those with  $(\lambda\mu)$  quantum numbers given by

$$\lambda + 2\mu = \lambda_0 + 2\mu_0 + N, \quad (1)$$

where  $\lambda_0$  and  $\mu_0$  denote labels of the leading SU(3) irrep in the  $0\hbar\Omega$  ( $N = 0$ ) subspace. We conjecture that this regular pattern of SU(3) quantum numbers reflects the presence of an underlying symplectic  $\text{Sp}(3, \mathbb{R})$  symmetry of microscopic nuclear collective motion [32] that governs the low-energy structure of both even-even and odd-odd

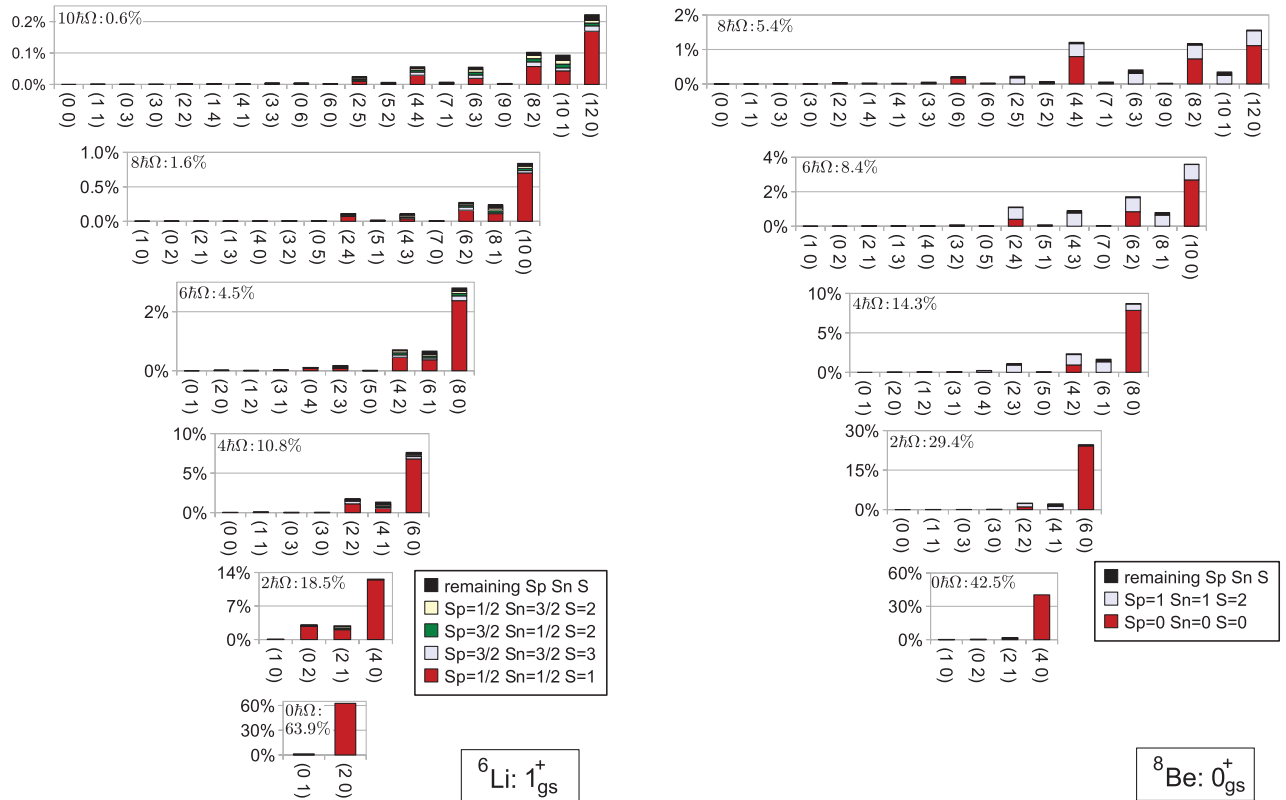


FIG. 1 (color). Probability distributions across  $(S_p S_n S)$  and  $(\lambda\mu)$  values (horizontal axis) for the calculated  $1_{\text{gs}}^+$  of  ${}^6\text{Li}$  obtained for  $N_{\text{max}} = 10$  and  $\hbar\Omega = 20$  MeV with the JISP16 interaction (left) and the  $0_{\text{gs}}^+$  of  ${}^8\text{Be}$  obtained for  $N_{\text{max}} = 8$  and  $\hbar\Omega = 25$  MeV with the chiral  $\text{N}^3\text{LO}$  interaction (right). The total probability for each  $N\hbar\Omega$  subspace is given in the upper left-hand corner of each histogram. The concentration of strengths to the far right demonstrates the dominance of collectivity.

$p$ -shell nuclei. This can be seen from the fact that  $(\lambda\mu)$  configurations that satisfy condition (1) can be determined from the leading SU(3) irrep  $(\lambda_0\mu_0)$  through a successive application of a specific subset of the  $\text{Sp}(3, \mathbb{R})$  symplectic  $2\hbar\Omega$  raising operators. This subset is composed of the three operators  $\hat{A}_{zz}$ ,  $\hat{A}_{zx}$ , and  $\hat{A}_{xx}$ , that distribute two oscillator quanta in the  $z$  and  $x$  directions, but none in the  $y$  direction, thereby inducing SU(3) configurations with ever-increasing intrinsic quadrupole deformation. These three operators are the generators of the  $\text{Sp}(2, \mathbb{R}) \subset \text{Sp}(3, \mathbb{R})$  subgroup [35], and give rise to deformed shapes that are energetically favored by an attractive quadrupole-quadrupole interaction [34]. This is consistent with our earlier findings of a clear symplectic  $\text{Sp}(3, \mathbb{R})$  structure with the same pattern (1) in *ab initio* eigensolutions for  $^{12}\text{C}$  and  $^{16}\text{O}$  [36].

Furthermore, the  $N\hbar\Omega$  configurations with  $(\lambda_0 + N\mu_0)$ , the so-called stretched states, carry a noticeably higher probability than the others. For instance, the  $(2 + N0)$  stretched states contribute at the 85% level to the ground state of  $^6\text{Li}$ , as can be readily seen in Fig. 1. The sequence of the stretched states is formed by consecutive applications of the  $\hat{A}_{zz}$  operator, the generator of  $\text{Sp}(1, \mathbb{R}) \subset \text{Sp}(2, \mathbb{R}) \subset \text{Sp}(3, \mathbb{R})$  subgroup, over the leading SU(3) irrep. This translates into distributing  $N$  oscillator quanta along the direction of the  $z$  axis only and, hence, rendering the largest possible deformation.

*Symmetry-guided framework.*—The observed patterns of intrinsic spin and deformation mixing supports the symmetry-guided basis selection philosophy referenced above. Specifically, one can take advantage of dominant symmetries to relax and refine the definition of the SA-NCSM model space, which for the NCSM is fixed by simply specifying the  $N_{\max}$  cutoff. In particular, SA-NCSM model spaces can be characterized by a pair of numbers  $\langle N_{\max}^{\perp} \rangle N_{\max}^{\top}$ , which implies inclusion of the complete space up through  $N_{\max}^{\perp}$ , and a subset of the complete set of  $(\lambda\mu)$  and  $(S_p S_n S)$  irreps between  $N_{\max}^{\perp}$  and  $N_{\max}^{\top}$ . Though not a primary focus of this Letter, an ultimate goal is to be able to carry out SA-NCSM investigations in deformed nuclei with  $N_{\max}^{\top}$  values that go beyond the highest  $N_{\max}$  for which complete NCSM results can be provided.

The SA-NCSM concept focuses on retaining the most important configurations that support the strong many-nucleon correlations of a nuclear system using underlying  $\text{Sp}(1, \mathbb{R}) \subset \text{Sp}(2, \mathbb{R}) \subset \text{Sp}(3, \mathbb{R})$  symmetry considerations. It is important to note that for model spaces truncated according to  $(\lambda\mu)$  and  $(S_p S_n S)$  irreps, the spurious center-of-mass motion can be factored out exactly [37], which represents an important advantage of this scheme.

The efficacy of the symmetry-guided concept is illustrated for SA-NCSM results obtained in model spaces which are expanded beyond a complete  $N_{\max}^{\perp}$  space with irreps that span a relatively few dominant intrinsic spin components and carry quadrupole deformation specified by Eq. (1). Specifically, we vary  $N_{\max}^{\perp}$  from 2 to 10 with

only the subspaces determined by Eq. (1) included beyond  $N_{\max}^{\perp}$ . This allows us to study convergence of spectroscopic properties towards results obtained in the complete  $N_{\max} = 12$  space and, hence, probes the efficacy of the SA-NCSM symmetry-guided model space selection concept. In the present study, a Coulomb plus JISP16  $NN$  interaction for  $\hbar\Omega$  values ranging from 17.5 up to 25 MeV is used, along with the Gloeckner-Lawson prescription [38] for elimination of spurious center-of-mass excitations. SA-NCSM eigenstates are used to determine spectroscopic properties of low-lying  $T = 0$  states of  $^6\text{Li}$  and the ground-state band of  $^6\text{He}$  for  $\langle N_{\max}^{\perp} \rangle 12$  model spaces.

The results indicate that the observables obtained in the  $\langle N_{\max}^{\perp} \rangle 12$  symmetry-guided truncated spaces are excellent approximations to the corresponding  $N_{\max} = 12$  complete-space counterparts. Furthermore, the level of agreement achieved is only marginally dependent on  $N_{\max}^{\perp}$ . In particular, the ground-state binding energies obtained in a  $\langle 2 \rangle 12$  model space represent approximately 97% of the complete-space  $N_{\max} = 12$  binding energy in the case of  $^6\text{Li}$  and reach over 98% for  $^6\text{He}$  [see Figs. 2(a) and 2(b)]. The excitation energies differ only by 5 to a few hundred keV from the corresponding complete-space  $N_{\max} = 12$  results [see Figs. 2(c) and 2(d)], and the agreement with known experimental data is reasonable over a broad range of  $\hbar\Omega$  values.

The number of basis states used, e.g., for each  $^6\text{Li}$  state, is only about 10%–12% for  $\langle 2 \rangle 12$ ,  $\langle 4 \rangle 12$ ,  $\langle 6 \rangle 12$ , 14% for  $\langle 8 \rangle 12$ , and 30% for  $\langle 10 \rangle 12$  as compared to the number for the complete  $N_{\max} = 12$  model space, which is  $3.95 \times 10^6$  ( $J = 1$ ),  $5.88 \times 10^6$  ( $J = 2$ ), and  $6.97 \times 10^6$  ( $J = 3$ ). The runtime of the SA-NCSM code exhibits a quadratic

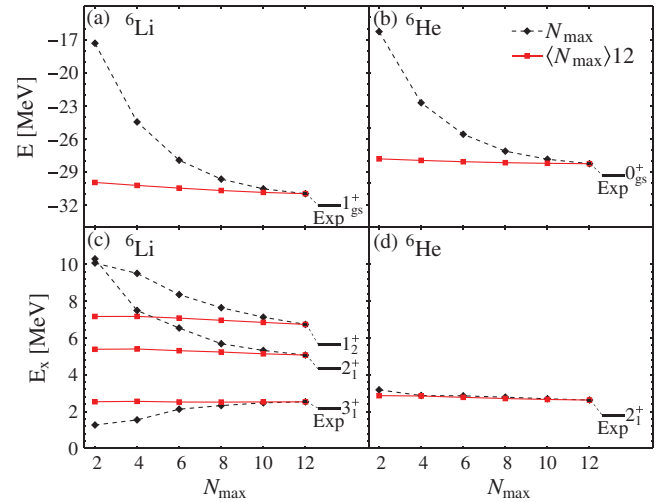


FIG. 2 (color). The ground-state binding energies of  $^6\text{Li}$  (a) and  $^6\text{He}$  (b), excitation energies of  $T = 0$  states of  $^6\text{Li}$  (c),  $2_1^+$  excited state of  $^6\text{He}$  (d), shown for the complete  $N_{\max}$  (dashed black curves) and truncated  $\langle N_{\max}^{\perp} = N_{\max} \rangle 12$  (solid red lines) model spaces. Results shown are for JISP16 and  $\hbar\Omega = 20$  MeV. Note the relatively large changes when the complete space is increased from  $N_{\max} = 2$  to  $N_{\max} = 12$  as compared to nearly constant  $\langle N_{\max} \rangle 12$  SA-NCSM outcomes.

TABLE I. Magnetic dipole moments  $\mu$  [ $\mu_N$ ] and point-particle rms matter radii  $r_m$  [fm] of  $T = 0$  states of  ${}^6\text{Li}$  calculated in the complete  $N_{\text{max}} = 12$  space and the  $\langle 6 \rangle 12$  subspace for JISP16 and  $\hbar\Omega = 20$  MeV. The experimental value for the  $1^+$  ground state is known to be  $\mu = +0.822 \mu_N$  [39].

		$1_1^+$	$3_1^+$	$2_1^+$	$1_2^+$
$\mu$	$N_{\text{max}} = 12$	0.838	1.866	0.970	0.338
	$\langle 6 \rangle 12$	0.839	1.866	1.014	0.338
$r_m$	$N_{\text{max}} = 12$	2.119	2.063	2.204	2.313
	$\langle 6 \rangle 12$	2.106	2.044	2.180	2.290

dependence on the number of ( $\lambda\mu$ ) and ( $S_p S_n S$ ) irreps for a nucleus—there are  $1.74 \times 10^6$  irreps for the complete  $N_{\text{max}} = 12$  model space of  ${}^6\text{Li}$ , while only 8.2%, 8.3%, 8.9%, 12.7%, and 30.6% of these are retained for  $N_{\text{max}}^\perp = 2, 4, 6, 8,$  and  $10$ , respectively. The net result is that calculations in the  $10 \geq N_{\text{max}}^\perp \geq 2$  range require 1 to 2 orders of magnitude less time than SA-NCSM calculations for the complete  $N_{\text{max}} = 12$  space.

As illustrated in Table I, the magnetic dipole moments obtained in the  $\langle 6 \rangle 12$  model space for  ${}^6\text{Li}$  agree to within 0.3% for odd- $J$  values, and 5% for  $\mu(2_1^+)$ . Qualitatively similar agreement is achieved for  $\mu(2_1^+)$  of  ${}^6\text{He}$ , as shown in Table II. The results suggest that it may suffice to include all low-lying  $\hbar\Omega$  states up to a fixed limit, e.g.,  $N_{\text{max}}^\perp = 6$  for  ${}^6\text{Li}$  and  $N_{\text{max}}^\perp = 8$  for  ${}^6\text{He}$ , to account for the most important correlations that contribute to the magnetic dipole moment.

To explore how close one comes to reproducing the important long-range correlations, we compared observables that are sensitive to the tails of the wave functions: specifically, the point-particle root-mean-square (rms) matter radii, the electric quadrupole moments, and the reduced electromagnetic  $B(E2)$  transition strengths that could hint at rotational features [40]. As Table II shows, the complete-space  $N_{\text{max}} = 12$  results for these observables are remarkably well reproduced by the SA-NCSM for  ${}^6\text{He}$  in the restricted  $\langle 8 \rangle 12$  space. In addition, the results for the rms matter radii of  ${}^6\text{Li}$ , listed in Table I, agree to within 1% for the  $\langle 6 \rangle 12$  model space.

Notably, the  $\langle 2 \rangle 12$  eigensolutions for  ${}^6\text{Li}$  yield results for  $B(E2)$  strengths and quadrupole moments that track closely with their complete  $N_{\text{max}} = 12$  space counterparts (see Fig. 3). It is known that further expansion of the model space

TABLE II. Selected observables for the two lowest-lying states of  ${}^6\text{He}$  obtained in the complete  $N_{\text{max}} = 12$  space and  $\langle 8 \rangle 12$  model subspace for JISP16 and  $\hbar\Omega = 20$  MeV.

	$N_{\text{max}} = 12$	$\langle 8 \rangle 12$
$B(E2; 2_1^+ \rightarrow 0_1^+) [e^2\text{fm}^4]$	0.181	0.184
$Q(2_1^+) [efm^2]$	-0.690	-0.711
$\mu(2_1^+) [\mu_N]$	-0.873	-0.817
$r_m(2_1^+) [\text{fm}]$	2.153	2.141
$r_m(0_1^+) [\text{fm}]$	2.113	2.110

beyond  $N_{\text{max}} = 12$  is needed to reach convergence [41,42]. However, the close correlation between the  $N_{\text{max}} = 12$  and  $\langle 2 \rangle 12$  results is strongly suggestive that this convergence can be obtained through the leading SU(3) irreps in a symmetry-adapted space. In addition, the results [see Fig. 3(c)] reproduce the ground-state quadrupole moment [43] that is measured to be  $Q(1^+) = -0.0818(17) efm^2$  [39].

The differences between truncated-space and complete-space results are found to be essentially  $\hbar\Omega$  insensitive and appear sufficiently small as to be nearly inconsequential relative to the dependences on  $\hbar\Omega$  and on  $N_{\text{max}}$  [see Fig. 3(b) and 3(d)]. Since the  $NN$  interaction dominates contributions from three-nucleon forces in light nuclei, except for selected cases [5–7], we expect our results to be robust and carry forward to planned applications that will include three-nucleon forces.

To summarize, the results reported in this Letter demonstrate that observed collective phenomena in light nuclei emerge naturally from first-principles considerations. This is illustrated through detailed calculations in a SA-NCSM framework for  ${}^6\text{Li}$ ,  ${}^6\text{He}$ , and  ${}^8\text{Be}$  nuclei using the JISP16 and chiral  $N^3\text{LO}$   $NN$  realistic interactions. The results underscore the strong dominance of configurations with large deformation and low spins. The results also suggest a path forward to include higher-lying correlations that are essential to collective features such as enhanced  $B(E2)$  transition strengths. The results further anticipate the significance of  $LS$  coupling and SU(3) as well as an underlying symplectic symmetry for an extension of *ab initio* methods to the heavier, strongly deformed nuclei of the lower  $ds$  shell, and, perhaps, even reaching beyond.

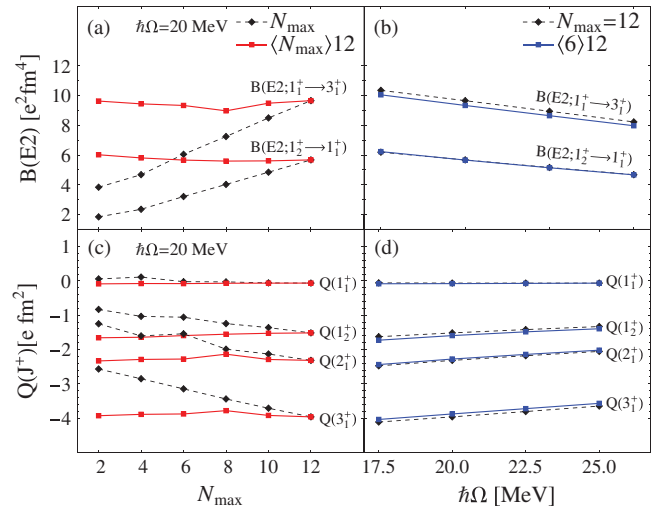


FIG. 3 (color). Electric quadrupole transition probabilities and quadrupole moments for  $T = 0$  states of  ${}^6\text{Li}$  calculated using the JISP16 interaction without using effective charges are shown for the complete  $N_{\text{max}}$  (dashed black lines) and truncated ( $N_{\text{max}}^\perp = N_{\text{max}} - 12$ ) (solid red lines) model spaces [(a) and (c)], and as a function of  $\hbar\Omega$  for the complete  $N_{\text{max}} = 12$  space and  $\langle 6 \rangle 12$  truncated space (solid blue lines) [(b) and (d)]. Experimentally,  $B(E2; 1_1^+ \rightarrow 3_1^+) = 25.6(20) e^2\text{fm}^4$  [39].

We thank David Rowe and Andrey Shirokov for useful discussions. This work was supported in part by the U.S. NSF [Grants No. OCI-0904874, No. OCI-0904809, and No. PHY-0904782], the US Department of Energy [Grants No. DESC0008485, No. DE-FG02-95ER-40934, and No. DE-FG02-87ER40371], the National Energy Research Scientific Computing Center [supported by the U.S. Department of Energy's Office of Science under Contract No. DE-AC02-05CH1123], the Southeastern Universities Research Association, and the Research Corporation for Science Advancement under a Cottrell Scholar Award. This work also benefitted from computing resources provided by the Louisiana Optical Network Initiative and Louisiana State University's Center for Computation & Technology. T.D. and D.L. acknowledge support from Michal Pajr and CQK Holding.

---

\*Present address: Department of Computer Science, University of North Carolina at Charlotte, Charlotte, North Carolina 28223, USA.

- [1] P. Sternberg, E. G. Ng, C. Yang, P. Maris, J. P. Vary, M. Sosonkina and H. V. Le, in *Proceedings of the 2008 ACM/IEEE Conference on Supercomputing, Austin, 2008*, (IEEE, New York, 2008), article number 15.
- [2] P. Maris, M. Sosonkina, J. P. Vary, E. G. Ng, and C. Yang, *Procedia Computer Science* **1**, 97 (2010).
- [3] H. M. Aktulga, C. Yang, E. N. Ng, P. Maris, and J. P. Vary, *Euro-par 2012, Lecture Notes on Computer Science* **7484**, 830 (2012).
- [4] P. Navrátil, J. P. Vary, and B. R. Barrett, *Phys. Rev. Lett.* **84**, 5728 (2000); *Phys. Rev. C* **62**, 054311 (2000).
- [5] B. R. Barrett, P. Navrátil, and J. P. Vary, *Prog. Part. Nucl. Phys.* **69**, 131 (2013).
- [6] P. Maris, J. P. Vary, P. Navrátil, W. E. Ormand, H. Nam, and D. J. Dean, *Phys. Rev. Lett.* **106**, 202502 (2011).
- [7] P. Maris, J. P. Vary, and P. Navrátil, *Phys. Rev. C* **87**, 014327 (2013).
- [8] R. B. Wiringa and S. C. Pieper, *Phys. Rev. Lett.* **89**, 182501 (2002).
- [9] G. Hagen, T. Papenbrock, D. J. Dean, and M. Hjorth-Jensen, *Phys. Rev. Lett.* **101**, 092502 (2008).
- [10] T. Neff and H. Feldmeier, *Nucl. Phys.* **A738**, 357 (2004).
- [11] S. Quaglioni and P. Navrátil, *Phys. Rev. Lett.* **101**, 092501 (2008).
- [12] S. K. Bogner, R. J. Furnstahl, P. Maris, R. J. Perry, A. Schwenk, and J. P. Vary, *Nucl. Phys.* **A801**, 21 (2008).
- [13] R. Roth, J. Langhammer, A. Calci, S. Binder, and P. Navratil, *Phys. Rev. Lett.* **107**, 072501 (2011).
- [14] E. Epelbaum, H. Krebs, D. Lee, and Ulf-G. Meissner, *Phys. Rev. Lett.* **106**, 192501 (2011); E. Epelbaum, H. Krebs, T. A. Lähde, D. Lee, and Ulf-G. Meissner, *Phys. Rev. Lett.* **109**, 252501 (2012).
- [15] P. Maris, A. M. Shirokov, and J. P. Vary, *Phys. Rev. C* **81**, 021301(R) (2010).
- [16] V. Z. Goldberg *et al.*, *Phys. Lett. B* **692**, 307 (2010).
- [17] B. Davids, R. H. Cyburt, J. Jose, and S. Mythili, *Astrophys. J.* **735**, 40 (2011).
- [18] A. M. Laird *et al.*, *Phys. Rev. Lett.* **110**, 032502 (2013).
- [19] A. M. Shirokov, J. P. Vary, A. I. Mazur, and T. A. Weber, *Phys. Lett. B* **644**, 33 (2007).
- [20] D. R. Entem and R. Machleidt, *Phys. Rev. C* **68**, 041001 (2003).
- [21] J. P. Elliott, *Proc. R. Soc. A* **245**, 128 (1958).
- [22] J. P. Draayer, T. Dytrych, K. D. Launey, and D. Langr, *Prog. Part. Nucl. Phys.* **67**, 516 (2012).
- [23] O. Castaños, J. P. Draayer, and Y. Leschber, *Z. Phys. A* **329**, 33 (1988).
- [24] G. Rosensteel and D. J. Rowe, *Ann. Phys. (N.Y.)* **104**, 134 (1977).
- [25] Y. Leschber and J. P. Draayer, *Phys. Lett. B* **190**, 1 (1987).
- [26] J. P. Draayer, *Nucl. Phys.* **A216**, 457 (1973).
- [27] N. Anantaraman, C. L. Bennett, J. P. Draayer, H. W. Fulbright, H. E. Gove, and J. Töke, *Phys. Rev. Lett.* **35**, 1131 (1975).
- [28] J. P. Draayer, *Nucl. Phys.* **A237**, 157 (1975).
- [29] J. P. Draayer, K. J. Weeks, and G. Rosensteel, *Nucl. Phys.* **A413**, 215 (1984).
- [30] G. Rosensteel, J. P. Draayer, and K. J. Weeks, *Nucl. Phys.* **A419**, 1 (1984).
- [31] J. P. Draayer and K. J. Weeks, *Phys. Rev. Lett.* **51**, 1422 (1983).
- [32] G. Rosensteel and D. J. Rowe, *Phys. Rev. Lett.* **38**, 10 (1977).
- [33] G. Rosensteel and D. J. Rowe, *Ann. Phys. (N.Y.)* **126**, 343 (1980).
- [34] D. J. Rowe, *Rep. Prog. Phys.* **48**, 1419 (1985).
- [35] D. R. Peterson and K. T. Hecht, *Nucl. Phys.* **A344**, 361 (1980).
- [36] T. Dytrych, K. D. Sviratcheva, C. Bahri, J. P. Draayer, and J. P. Vary, *Phys. Rev. Lett.* **98**, 162503 (2007).
- [37] B. J. Verhaar, *Nucl. Phys.* **A21**, 508 (1960).
- [38] D. H. Gloeckner and R. D. Lawson, *Phys. Lett.* **53B**, 313 (1974).
- [39] D. R. Tilley, C. M. Cheves, J. L. Godwin, G. M. Hale, H. M. Hofmann, J. H. Kelley, C. G. Sheu, and H. R. Weller, *Nucl. Phys.* **A708**, 3 (2002).
- [40] M. A. Caprio, P. Maris, and J. P. Vary, *Phys. Lett. B* **719**, 179 (2013).
- [41] C. Cockrell, J. P. Vary, and P. Maris, *Phys. Rev. C* **86**, 034325 (2012).
- [42] P. Maris and J. P. Vary, *Int. J. Mod. Phys. E* **22**, 1330016 (2013).
- [43] The near vanishing of the quadrupole moment, an  $L = 2$  object, in the ground state of  ${}^6\text{Li}$ ,  $Q(1_1^+)$ , can be attributed to a very strong dominance ( $\sim 87\%$ ) of  $L = 0$  configurations in the ground state.